Stereoelectronic Influence of a "Spectator" Propargylic Substituent Can Override Aromaticity Effects in Radical *Peri*-cyclizations on Route to Expanded Polyaromatics.

Audrey M. Hughes, Gabriel dos Passos Gomes, Igor V. Alabugin*

Department of Chemistry and Biochemistry, Florida State University, Tallahassee, FL, 32306, USA. Email: alabugin@chem.fsu.edu

Table of Contents Graphic

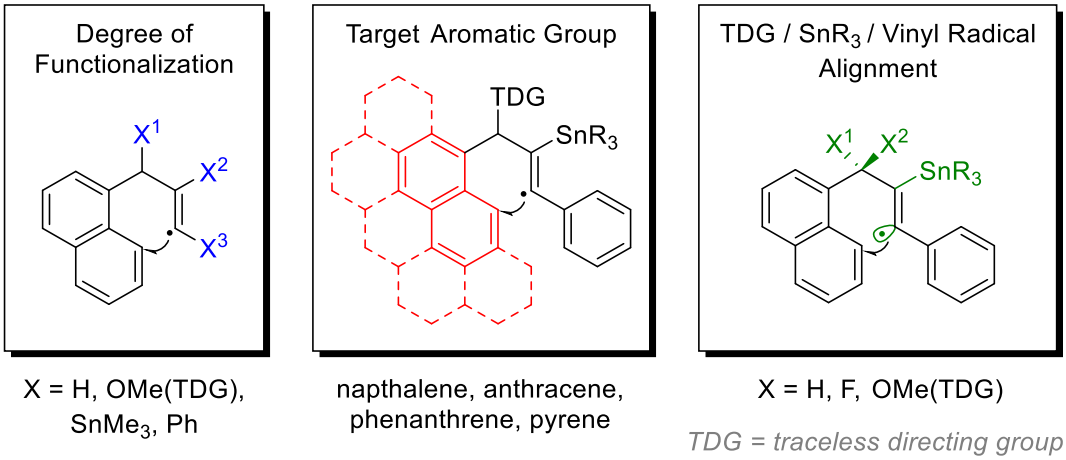

Abstract

Computational analysis quantifies key trends in "*peri*-" radical cyclizations, a recently developed process for benzannulation at the zigzag edge. The key novel finding is the unprecedented sensitivity of *peri*-cyclization to the presence and spatial orientation of a "spectator" propargylic -OMe substituent. Remarkably, formation of *cis*-products proceeds, in general, through a significantly (~2-4 kcal/mol) lower barrier than formation of the *trans*-products, even when the *cis*-products are less stable. The origin of this unexpected effect is clearly stereoelectronic. These findings identify such remote substitution as a conceptually new tool for the control of rate and selectivity of radical reactions.

The correlations of activation barriers for vinyl radical attack with aromaticity of the target shows the expected relationship in phenanthrenes and pyrenes but not in anthracenes. In the latter case, the attack at the less aromatic ring corresponds to a higher barrier because a steric penalty on

the stereoelectronically favorable *cis*-TS negates the accelerating influence of the properly aligned C-O and C-Sn bonds.

Introduction

Benzannulative expansion of polyaromatic systems is an effective method of creating graphene substructures.[1] The high carbon content and energetic properties of alkynes makes them convenient building blocks for creating expanded cyclic structures[2] (Figure 1).

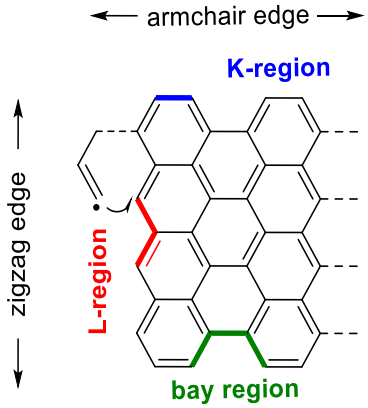

Figure 1. Graphene edge types and sites of reactivity with a *peri*-radical annulation at the zigzag edge.

Success in making graphene ribbons and flakes of the desired sizes and shapes, depends on the absence of structural defects, such as heteroatoms, sp^3-hybridized centers, and five-membered rings, can disrupt the perfect honeycomb pattern of graphene fragments.

Radical cascades offer an atom-economical approach towards the preparation of functionalized polyaromatics. Earlier, we have reported a number of alkyne-mediated radical cascades initiated via selective attack by a tin radical on the central alkyne of an oligoalkyne precursor.[3] The initial attack was followed by a series of 6-exo cyclizations to provide a fully cyclized polyaromatic ribbon. Two structural defects, inherent to the nature of this cascade, have been addressed in a series of design modifications. In particular, the use of skipped, rather than fully conjugated, oligoalkynes allowed to avoid incorporation of a five-membered ring at the initiation point (Figure 2).[4] Formation of a 5-membered cycle at the last C-C bond formation at the end of the cascade can be avoided in two ways: 1) by deactivating the radical to the extent

where it is incapable of attacking the terminal aryl ring and the last cyclization is aborted,[5] or 2) by using a cyclization at the *peri*-position of a naphthalene subunit as the last cycle-forming step.

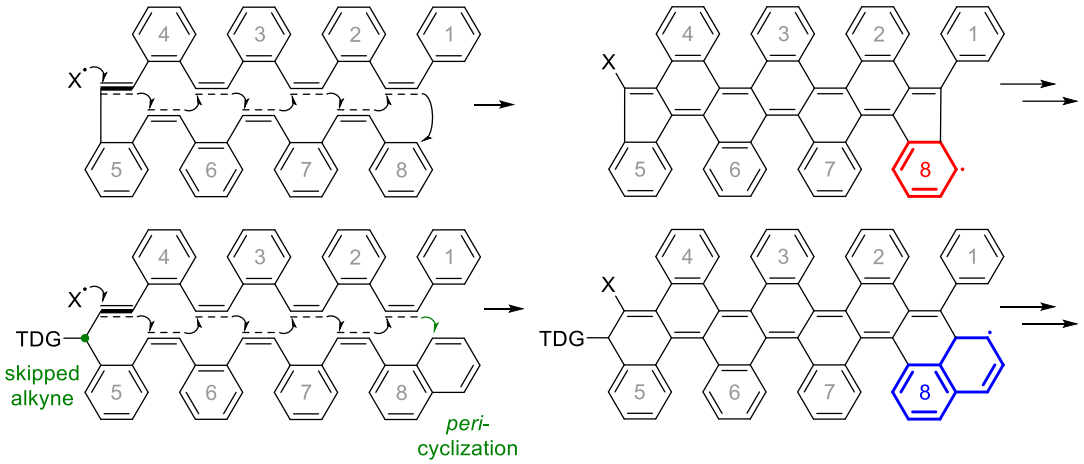

***Figure 2**. Top: the problem of two pentagonal "defects" in the preparation of polyaromatic ribbons from conjugated oligoalkynes. Bottom: Two structural design elements that help to avoid formation of five-membered rings: initiation from a skipped alkyne equipped with a traceless directing group and termination via a "*peri*-" cyclization. (TDG=Traceless Directing Group).*

Because radical *peri*-cyclizations have been unknown until recently,[6] we explored their viability using several polyaromatic targets with the zigzag edge as partners in the *peri*-cyclizations with an appropriately positioned vinyl radical.

Vinyl radical attack at the *peri*-position of a polyaromatic target allows for cascade termination with 6-membered cycles. The initially formed products are unstable and the reaction requires either oxidative or reductive termination. For the anthracene substrate, the oxidative workup provides benzo[*de*]anthracenones (Scheme 1). Alternatively, reductive termination produced benzo[*de*]anthracenes in yields of 56-65%.

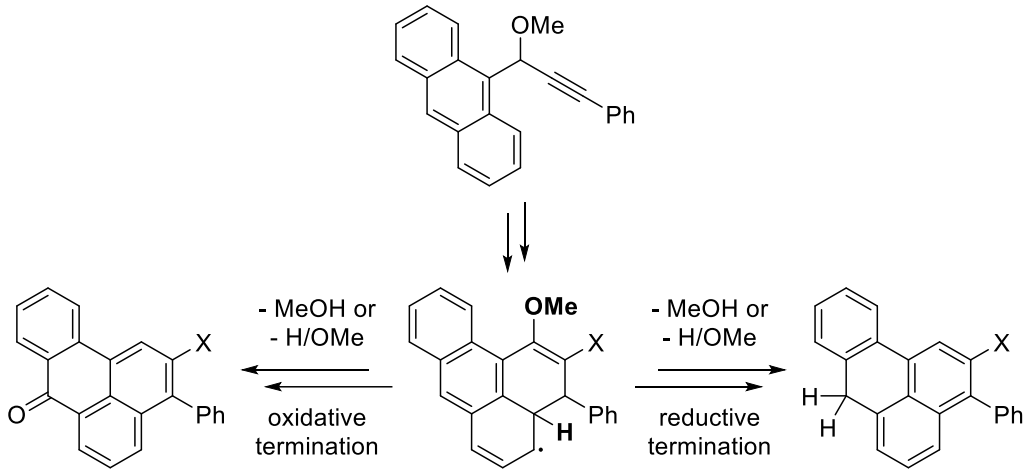

Scheme 1. An example of *peri*-cyclization on an anthracene core and the products of oxidative and reductive workups.

The purpose of this paper is to use computational analysis to understand the energetics of *peri*-cyclizations of vinyl radicals, their dependence on the nature of the polyaromatic core as well as on substitution at the radical center and at the propargylic carbon (Figure 3).

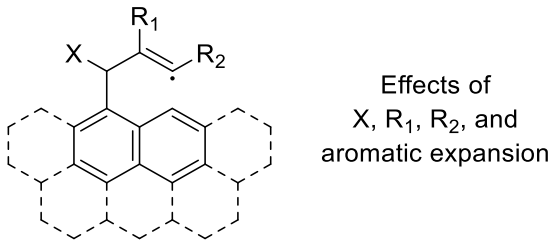

Figure 3. The scope of computational analysis of peri-cyclizations.

Results and Discussion

Parent examples for the *peri*- and *ortho'*-cyclization of naphthalene and biphenyl[7] were examined first to establish a point of reference for expanded systems (Scheme 2). Although a methoxy group cannot be added to the biphenyl substrate to fully resemble the cyclization precursor for the naphthalene system, effect of substitution at the vinyl radical can be compared for both types of cyclizations in order to gain better understanding of electronic factors for the attack at armchair and zigzag edges of a polyaromatic system. These effects were modeled by using an unsubstituted vinyl radical, an α-Ph-substituted radical, and an α-Ph-β-$SnMe_3$-

disubstituted radical as the cyclization precursors for both the biphenyl and the naphthalene systems (Scheme 2).

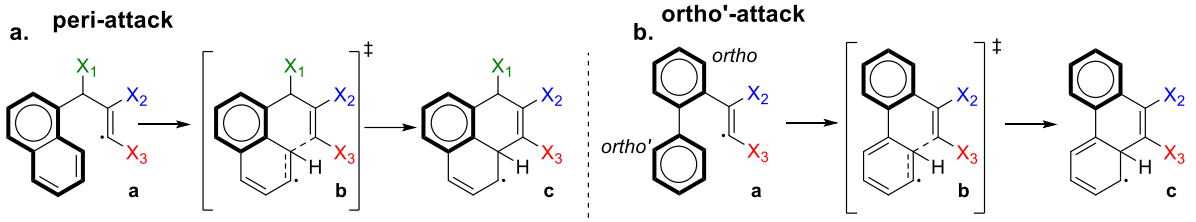

1:	X_1 = H X_2 = H X_3 = H	$\Delta H^{\ddagger}$ = +8.8 **$\Delta G^{\ddagger}$ = +11.4**	ΔH = -28.6 **ΔG = -26.0**	4:	X_2 = H X_3 = H	$\Delta H^{\ddagger}$ = +6.5 **$\Delta G^{\ddagger}$ = +8.6**	ΔH = -25.9 **ΔG = -23.4**
2:	X_1 = H X_2 = H X_3 = Ph	$\Delta H^{\ddagger}$ = +9.4 **$\Delta G^{\ddagger}$ = +12.2**	ΔH = -20.7 **ΔG = -16.9**	5:	X_2 = H X_3 = Ph	$\Delta H^{\ddagger}$ = +7.0 **$\Delta G^{\ddagger}$ = +9.3**	ΔH = -18.8 **ΔG = -15.4**
3:	X_1 = H X_2 = $SnMe_3$ X_3 = Ph	$\Delta H^{\ddagger}$ = +12.1 **$\Delta G^{\ddagger}$ = +13.0**	ΔH = -14.7 **ΔG = -10.7**	6:	X_2 = $SnMe_3$ X_3 = Ph	$\Delta H^{\ddagger}$ = +6.5 **$\Delta G^{\ddagger}$ = +10.7**	ΔH = -14.2 **ΔG = -8.2**

Scheme 2. Comparison of substituent effects in the vinyl radical cyclization at *peri*-position of a) naphthalene and b) *ortho'*-positions of biphenyl (see Figure S1 for additional examples).

For all of the cyclization pairs with analogous substitution, the more flexible biphenyl system has a lower transition state despite being less exergonic. This observation suggests that flexibility, or lack thereof, may play a role in the reactivity of the polyaromatic cores. For a more rigid fused naphthalene core, the geometric distortion needed for the radical attack at the π-system is more energetically costly.

Substituent effects: direct substitution at the alkyne. Radical-stabilizing substituents near the vinyl center increase both the activation barriers and reaction energies. For both *peri*- and *ortho'*-attack, the presence of a phenyl group at the α-position and then a trimethyl tin at the β-position increased the activation barrier by ~2 kcal/mol overall. The reaction exergonicities decrease even more dramatically by ~15 kcal/mol. In general, *ortho'*-cyclizations are slightly less affected by substitution at the vinyl radical than *peri*-cyclizations; and transition states are much less affected by substitution than are the products.

The correlation of ΔG and $\Delta G^{\ddagger}$ for the three substituent combination in each of the cyclization patterns shows that the differences in the activation barrier are due to the radical

stabilization effects that decreased exergonicity of the radical attack. Both the α-Ph group and the β-Sn substituent substantially stabilize the reacting radical.[8]

The stabilizing effect of the two substituents is preserved in the transition state as illustrated by Figure 4 where both the C-Sn bond and the Ph group π-systems are aligned well with the attacking radical center:

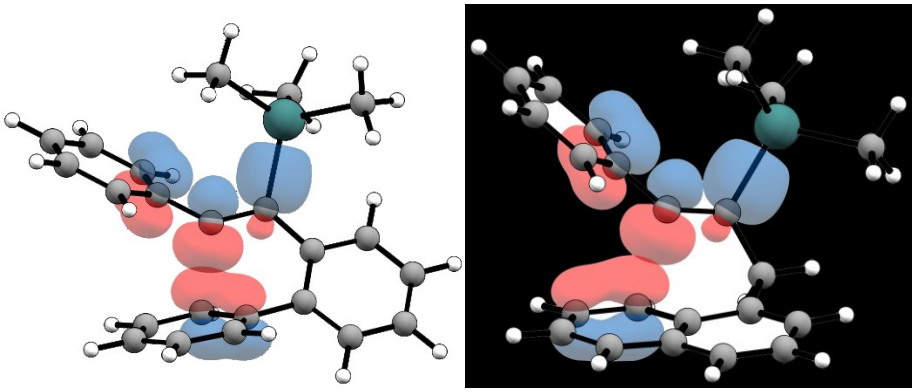

Figure 4. Transition states of α-Ph-β-$SnMe_3$-disubstituted biphenyl **6b** and naphthalene **3b**, illustrating the key orbitals interacting with the radical center.

Indirect substituent effects: **Presence and orientation of an OMe group at the propargylic carbon.** Due to the essential role of the methoxy group in directing the tin radical attack at the alkyne, we analyzed the cyclization of OMe-substituted substrates. Remarkably, the outcome of the cyclization depended dramatically on the orientation of the "spectator" propargylic substituents. Considering our long-standing interest in stereoelectronic control of organic reactions,[8d, 9] including the effects of remote substituents,[10] we have analyzed this situation in more detail as discussed below.

The introduction of a methoxy group at the propargyl position leads to interesting effects that depend strongly on the orientation of this substituent (Scheme 3). The activation enthalpy for the cis transition state **7b** is 1.5 kcal/mol lower than for the transition state **3b** that lacks the propargylic substituent, whereas the activation barrier for the trans transition state (**7b-t**) is 3.6 kcal/mol higher. Entropic factors change the magnitude of effects slightly but the large (4.3 kcal/mol) influence of remote substituent on the free energy barriers persists. The magnitude of this effect is remarkable for a group that is attached directly neither to the vinyl radical moiety nor to the aromatic target. What makes this observation even more interesting is that the difference in

the reaction free energies (1.6 kcal/mol) is significantly smaller than the difference in the activation barriers, indicating that the observed barrier differences may stem from specific transition state stabilization.

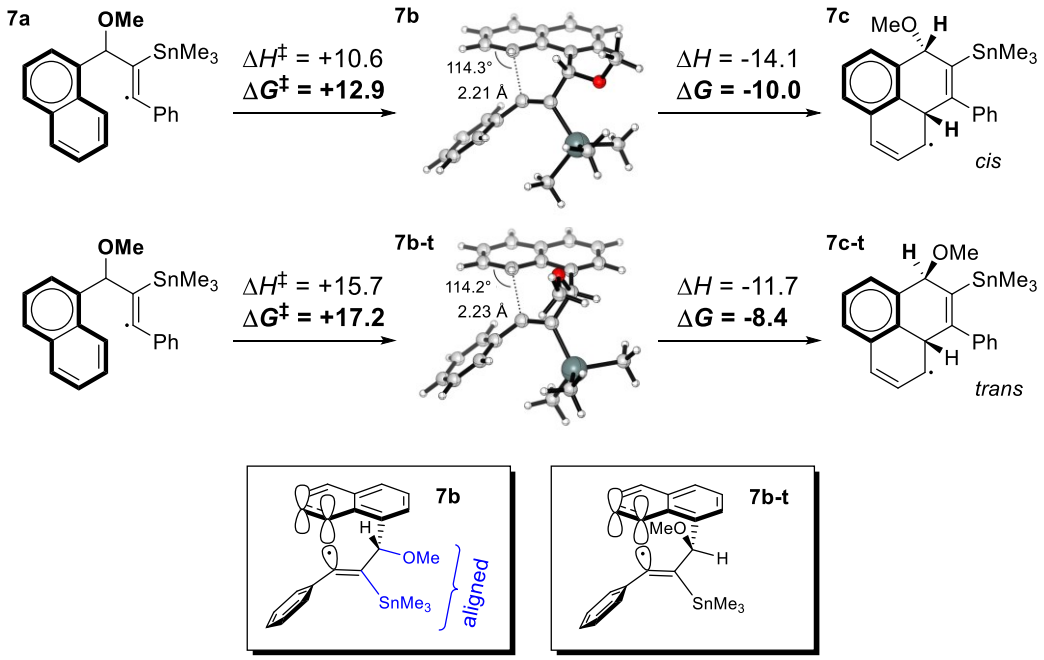

Scheme 3. The large effect of propargylic substituent at the activation barrier for the *peri*-cyclization at naphthalene. The transition state energies are given relative to the most stable conformer of the reactant in the spirit of the Curtin-Hammett principle.

In the subsequent sections, we expand the list of polyaromatic targets to test whether these stereoelectronic factors are general and operate in the broader family of *peri*-cyclizations

Effect of the aromatic target. The expansion of the aromatic system and change in the targeted ring attack leads to noticeable differences in the computed barriers and reaction energies for the radical cyclizations. However, the stereoelectronic effect of the propargylic -OMe group persisted. We will discuss it in the following sections. Herein, we will concentrate our analysis at the lower energy path that leads to the formation of *cis*-products. It is instructive to compare cyclizations at naphthalene with cyclizations at the two *peri*-positions of anthracene, at carbons 9 and 1 (Scheme 4). The results are non-trivial – the *peri*-attack at the anthracene ring can be slower or faster than the attack in the naphthalene system depending on which anthracene ring is targeted. The effects

are large. Compared to the cyclization in naphthalene, the free energy of activation is 4.5 kcal/mol lower for the 9th position of anthracene and 1.3 kcal/mol higher for the 1st position of anthracene.

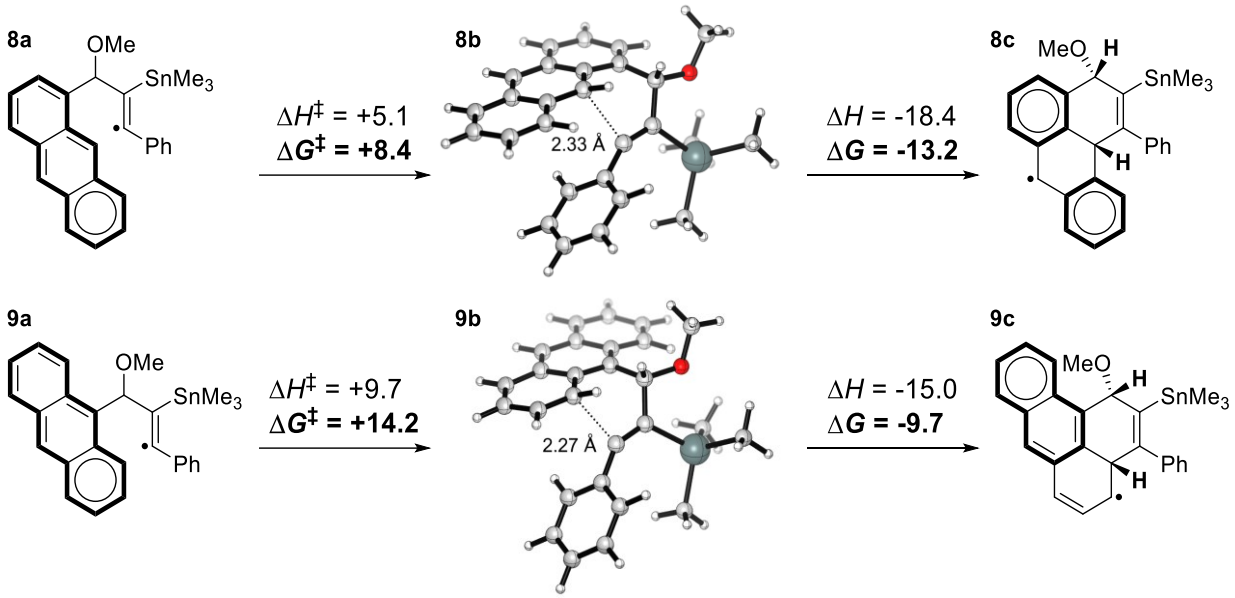

Scheme 4. The vinyl radical cyclization in 1-naphthalene **7a**, 1-substituted anthracene **8a,** and 9-substituted anthracene **9a**.

The faster attack at the 9th position (i.e., the central ring) in the 1-substituted anthracene **8a** should not be surprising. Two isolated Clar's sextets are maintained in the product, and their conjugation is possible through the one-carbon bridge. In the second anthracene isomer **9a**, attack proceeds at the terminal ring to transform the anthracene moiety into a β-allyl naphthalene π-system. It is reasonable to expect this process to be less favored than attack at the central anthracene ring, but it is unclear why it is also less favored than attack at the naphthalene ring of **7a**. A closer inspection reveals that part of the problem with the terminal attack in **9a** is due to the unfavorable entropic contribution. We will come back to this seemingly anomalous behavior later.

Radical additions to the phenanthrenes was analyzed next. Here the results followed the known trends in reactivity of the phenanthrene subunits. Attack at the less aromatic central ring was significantly more exergonic and proceeded via a lower barrier.

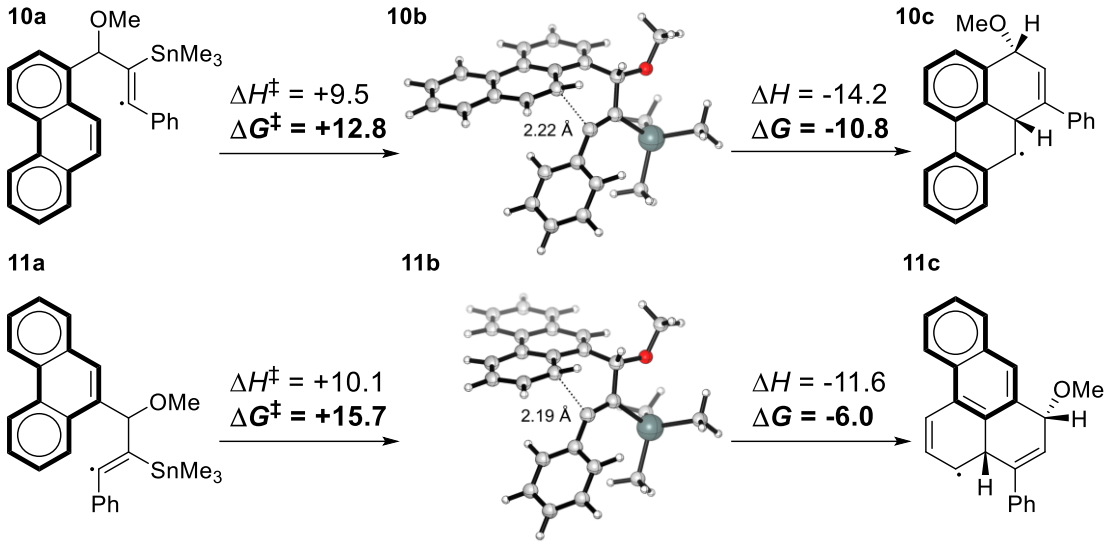

Scheme 5. The vinyl radical cyclization in 1-phenanthrene **10a** and 9-phenanthrene **11a** structures.

In particular, when the central double bond is attacked in 1-phenanthrene **10**, the reaction is downhill by 11 kcal/mol (Scheme 5). After the attack, the π-system of biphenyl is formed, similar to that for anthracene **9a**. Attack at the outer aromatic ring in **11** is less favorable thermodynamically and proceeds through a 3 kcal/mol higher barrier. After the attack, the cyclization product contains an α-allyl naphthalene substructure.

Finally, additions to pyrenes generally display trends that are similar to additions to phenanthrenes, reflecting the electronic similarity between the two aromatic systems (Scheme 6). Similar to the phenanthrene example, attack at the weaker central double bond 1-pyrene **12a** is more favorable. This process forms a radical that contains phenanthrene, a relatively stable polyaromatic fragment. On the other hand, when the terminal ring of **13a** is attacked, the barrier and reaction energy are slightly higher by 1.3 kcal/mol and 1.9 kcal/mol, respectively. A naphthalene and phenalenyl resonance subunits can be discerned in the product of this attack.

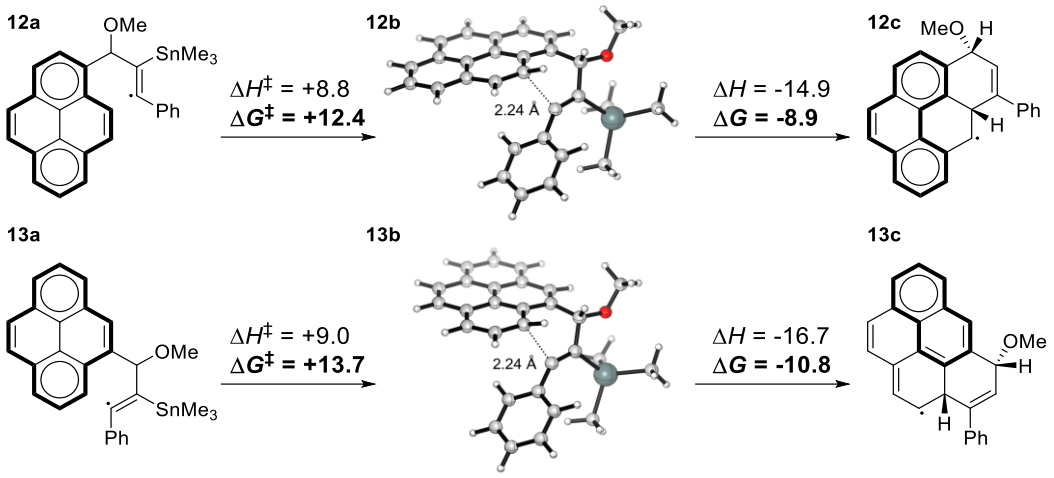

Scheme 6. The vinyl radical cyclization in 1-pyrene **12a** and 4-pyrene **13a** structures; phenalenyl resonance form of the 4-pyrene product**.**

We have also calculated barriers and reaction energies for the radical cyclizations that yield the *trans*-products (Scheme 7). Again, the reactions are considerably less favorable kinetically that analogous reactions that yield the *cis*-products. The only exception is the radical attack at the terminal ring in the reaction of 9-substituted anthracene substrate where the difference in the calculated *cis*- and *trans*-activation barriers is very small. However, even in the latter case the *trans*-product formation remained ~0.1 kcal/mol l*ess favorable kinetically* despite being >3 kcal/mol *more favorable thermodynamically*.

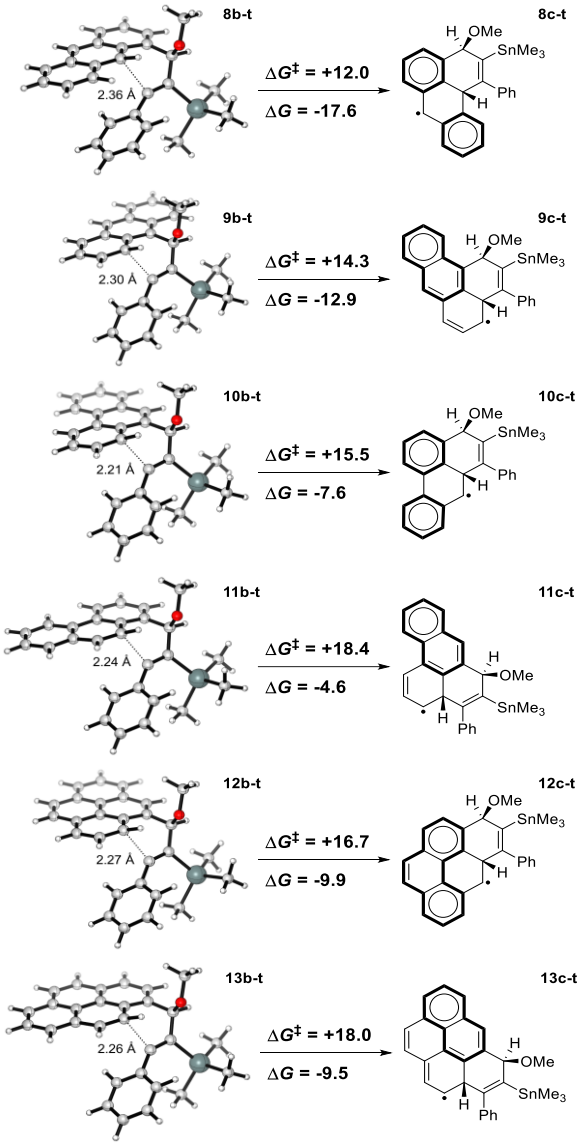

Scheme 7. Calculated reaction free energies and barriers for radical *peri*-cyclizations that form the *trans*-products.

This deviation from the general trend in the 9-anthracenes can be attributed to steric interactions that are not present in the other compounds (Figure 5). In both the starting materials and the *cis*-transition state, the methoxy group is not able to attain the favorable alignment with the C-Sn bond without clashing with the C-H bond at the other *peri*-position. This unfavorable steric interaction nearly completely compensates for the favorable stereoelectronics of the *cis*-transition state. As the result, the *cis*- and *trans*-*peri*-cyclizations in the 9-anthracene system have almost identical barriers.

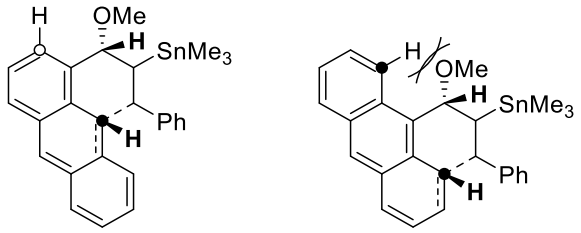

cis 1-anthracene (8b)
(one *ortho*- and one *peri*- C-H)

cis 9-anthracene (9b)
(two *peri*- C-H)

Figure 5. Steric effect on the cis-radical attack in the two anthracenes (see SI for stability comparison of isomers).

The role of aromaticity. Considering the well-known role of aromaticity in stability and reactivity of organic molecules,[8d,11] we have also explored whether the variations in aromatic character of different rings of polycyclic aromatics will have an effect on the reaction energies and barriers of *peri*-cyclizations. Aromaticity is a complex phenomenon described via an interplay of energetic, structural, and magnetic effects that do not often correlate perfectly with each other. In this work, we chose to use the NICS method developed by Schleyer, et al.[12] as a quantitative indicator of aromaticity. This method was shown to provide valuable information for a variety of aromatic systems in the ground, transition, and excited states.[13]

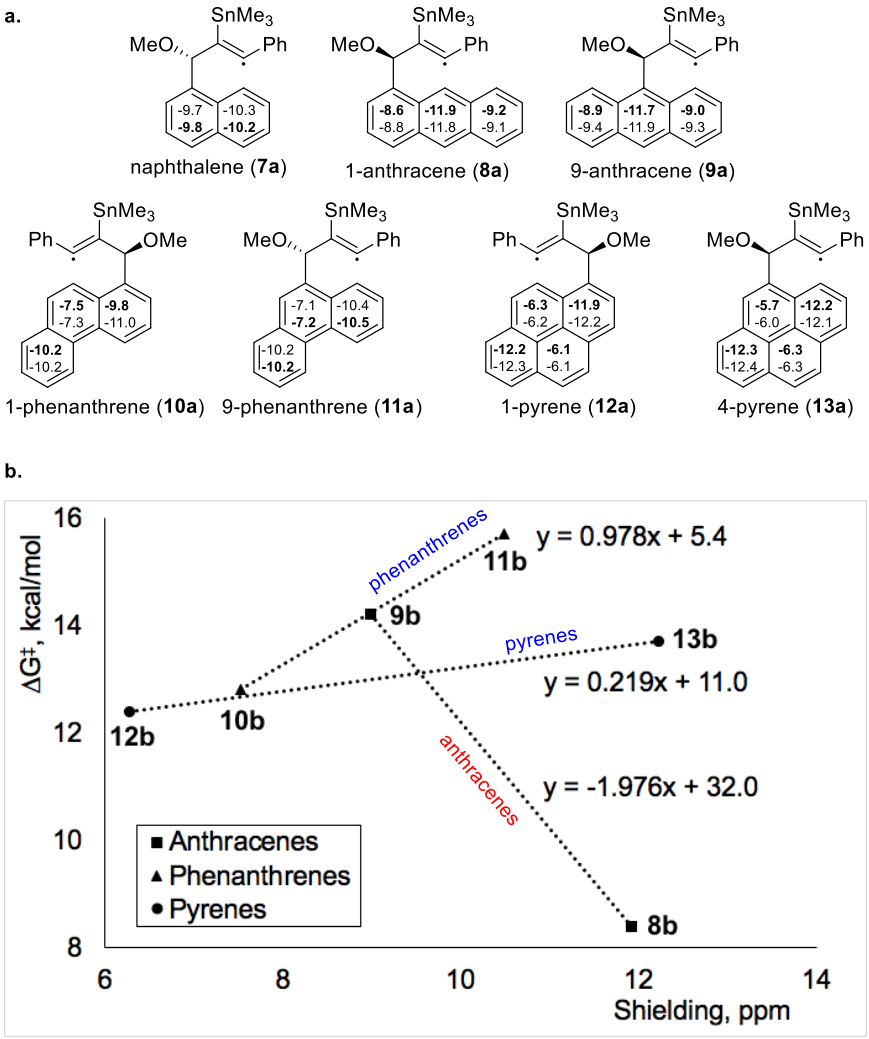

Figure 6. a) NICS(1) of vinyl radical species, bolded values represent the face attacked to form 6-membered *cis*-products, and b) aromaticity vs. reaction barrier for corresponding starting materials above.

NICS(1) values for both faces of each ring in the vinyl radical species were compared (Figure 6). NICS(1) can be used as an indicator of aromaticity[13b] as a function of calculating shielding above and below a ring. For the phenanthrene and pyrene pairs of cyclizations that target the same core, but at different positions, the lower barrier correlates to the attack at the less aromatic ring. Additionally, the effect of aromaticity in comparing phenanthrene and pyrene seems to diminish with the increase from three to four rings in the core. Aromaticity in smaller phenanthrene systems had a larger effect on reaction barriers, where the larger pyrene systems had a smaller effect. However, for attack at the anthracene ring system, other factors seem to override

this pattern, and the lower barrier is associated with attack at the more aromatic ring. The 1-anthracene reaction is the more facile of the two despite the fact that the stronger ring is broken, and there is a large negative correlation between aromaticity and reaction barrier. This suggests that aromaticity at the site of attack is not an absolute predictor of reaction energies.

Stereoelectronic effects in *peri*-cyclizations. As the previous part illustrates, the effects of aromaticity can be overridden by other factors. In this section, we show that these observations stem from the stereoelectronic factors associated with the relative position of the -OMe and the -SnR_3 group.

As we discussed above, the lower energy transition state for the *peri*-addition to naphthalene has the OCCSn dihedral of 1.4° where the -OMe and C-Sn bonds are syn-*peri*planar. In contrast, the -OMe and C-Sn bonds are nearly orthogonal in the higher energy transition state. The same trend is observed for all of the other polyaromatic targets.

It is appealing to attribute this unexpected but general effect to the clear stereoelectronic differences between the two transition states. In the lower energy transition state, the $\sigma_{C\text{-}OMe}$ bond and the radical orbital are aligned with the "relay" C-Sn orbital whereas in the higher energy transition state, the $\sigma_{C\text{-}OMe}$ bond is nearly orthogonal to the radical and to the vinyl C-Sn bond. One can suggest that the syn-*peri*planar arrangement of the C-O and C-Sn bonds can lead to partial electron density transfer from the C-Sn bond,[3a] rendering the latter a weaker hyperconjugative donor towards the vinyl radical. In turn, the decreased electron donation to the radical center renders the latter more electrophilic and more reactive towards the electron-rich π-cloud of naphthalene. In the higher energy stereoisomeric transition state, the C-O and C-Sn are nearly orthogonal, so electron density is not drained from the C-Sn bond via σ-conjugation. Instead, the C-Sn bond can fully exert its donor effect on the vinyl radical, deactivating it towards radical attack. An additional deactivating effect that may complement the primary effect discussed above is the alignment of the C-O acceptor with the π-system of the naphthalene. In the higher energy transition state, this alignment can transfer electron density from the naphthalene, rendering the latter less nucleophilic.

In this scenario, the C-O bond serves as a stereoelectronic gate: in the lower energy transition state, it deactivates the C-Sn donor and restores electrophilicity of the vinyl radical. In

the higher energy transition state, the C-Sn donor lowers electrophilicity of the vinyl radical while the C-O bond lowers nucleophilicity of the π-target.

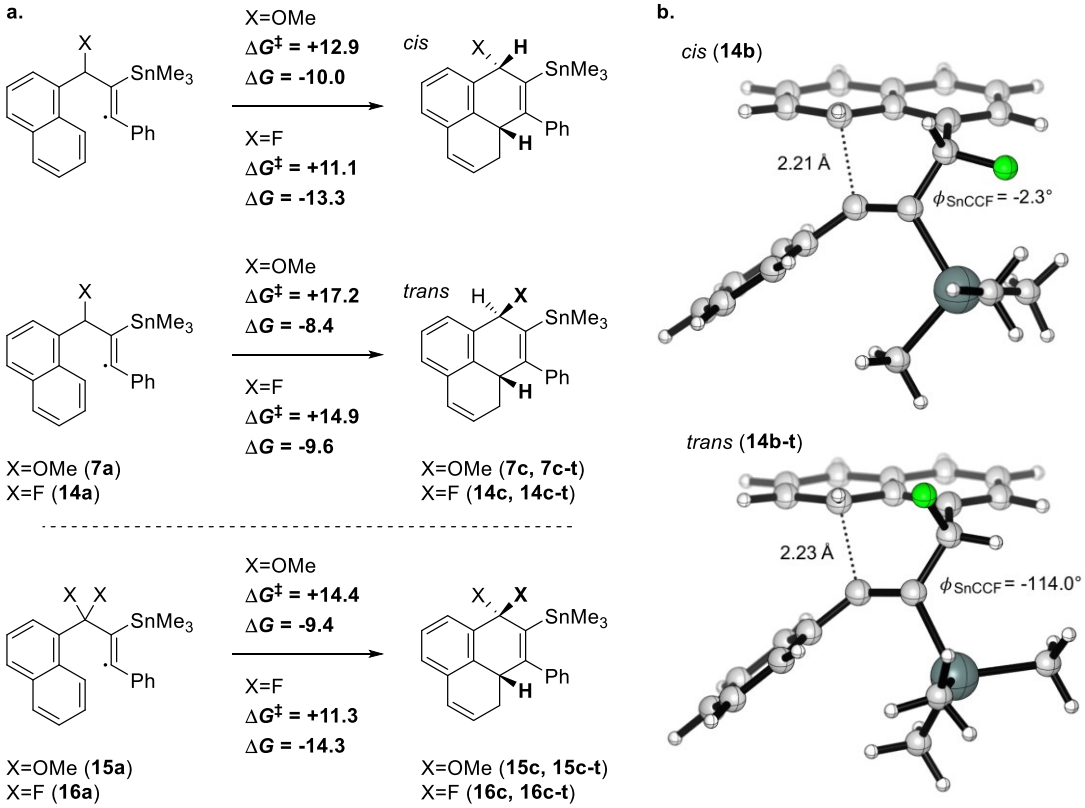

Scheme 8. The role of propargylic substituents in reactivity: comparison of C-O and C-F bonds. a) Barriers and reaction energies. b) Comparison of geometries for the cis- and trans-isomer formation.

To test for the role of sigma acceptor ability of the propargylic substituent, we have changed the C-OR group to a C-F bond (Scheme 8). Indeed, the stronger sigma acceptor accentuated the energy difference between the two transition states. The difference now is 3.7 kcal/mol. The transition state energy lowering relative to the unsubstituted case illustrates the activating role of these orbital interactions.

Adding another acceptor (**15a**, **16a**) is counter-productive – the barriers go up relative to the stereoelectronically aligned systems with a single propargylic substituent. This finding further underscores the stereoelectronic origin of this effect since the second acceptor in the disubstituted systems cannot be aligned properly with the C-Sn bond and the radical center.

Note that we took advantage of the Curtin-Hammett principle and reported the barriers as the energy difference between the lowest energy TS (cis) and the most stable conformer of the reactant (syn).[14] Since the the donor-acceptor interactions in the syn-geometry benefit more from a stronger acceptor (X=F), the difference in the activation barriers is increased by the introduction of a fluorine atom.

Table 1. Natural Bond Orbital (NBO) analysis of **7b**, **7b-t**, **14b**, and **14b-t** and their corresponding starting materials. Second order perturbation energies for the orbital interactions are given in kcal/mol.

		Methoxy			Fluorine		
interaction	Spin	vinyl radical	*cis*-TS	*trans*-TS	vinyl radical	*cis*-TS	*trans*-TS
$\sigma_{C\text{-}Sn} \rightarrow \sigma^*_{C\text{-}X}$	α	2.3	2.1	0.9	2.7	2.9	0.9
	β	2.5	2.1	0.9	2.8	2.9	0.9
$n_X \rightarrow \sigma^*_{Sn\text{-}CH_3}$	α	1.9	1.4	0	1.3	1.3	0
	β	1.9	1.5	0	1.3	1.3	0
$\sigma_{C\text{-}Sn} \rightarrow$ vinyl radical	β	31.2	29.0	28.7	29.8	28.8	28.7

We have further evaluated the role of suggested orbital interactions using Natural Bond Orbital (NBO) analysis (Table 1). This analysis suggests that stabilization provided by the alignment of -OMe/-F and -$SnMe_3$ partially stems from the $\sigma_{C\text{-}Sn} \rightarrow \sigma^*_{C\text{-}X}$ interaction. Whereas both the most stable conformer of the reacting vinyl radical and the more stable *cis*-TS maintain this stabilizing interaction, this effect weakens significantly in the *trans*-TS (from ~4-5 to ~2 kcal/mol). Unexpectedly, NBO analysis suggests that additional stabilization to the *cis*-TS comes from the direct through-space donation from the lone pair of oxygen to the $\sigma^*_{Sn\text{-}CH_3}$ orbital (~ 3 vs. 0 kcal/mol for *cis*- vs. *trans*-). Interestingly, these two donor-acceptor hyperconjugative effects balance density redistribution due to the interaction of O- and Sn-containing moieties in a way that maintains the donor ability of the C-Sn bond towards the vinyl radical ($\sigma_{C\text{-}Sn} \rightarrow$ vinyl radical interaction) relatively constant. In this NBO description, the geometric changes in the OCCSn

system do not considerably perturb the vinyl radical reactivity, modifying the stereoelectronic model suggested earlier.

Analysis of the 5-membered cycle formation. Finally, we have evaluated the possibilibity of an alternative cyclization route – the five-membered ring formation by the ortho-attack of the vinyl radical (Scheme 9). The calculated barrier is much higher, suggesting that this process is unlikely to be important from the experimental point of view and explaining why the peri-cyclizations work relatively well.

Interestingly, the stereoelectronic preference for the cis-TS is observed for the formation of the 5-membered rings as well. This finding is noteworthy in the naphthalene system where the formation of cis-isomer is ~2 kcal/mol endergonic while the formation of the trans-isomer is thermoneutral. However, the difference in the cis- and trans-cyclization barriers is much lower because attaining the favorable co-planar arrangement of CO and CSn bonds is more difficult in the smaller, more strained five-membered ring. In accord with this notion, the SnCCO dihedral in the cis-TS in the naphthalene system is ~21 degree – a noticeable deviation from coplanarity.

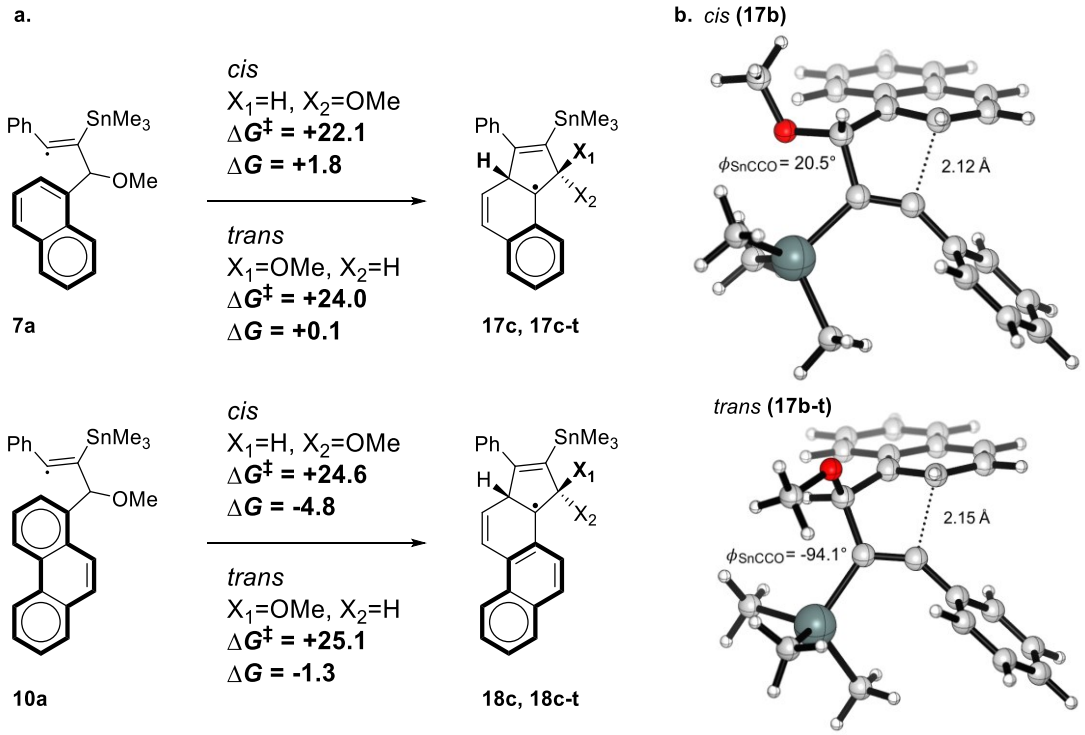

Scheme 9. a) Barriers and reaction energies for 5-membered ring formation in the naphthalene and phenathrene systems. b) Comparison of geometries for the *cis*- and *trans*-isomer formation in the naphthalene and phenathrene system.

Comparison of alkyne and *peri*-cyclizations. In conclusion, it is interesting to compare the two similar ways for the annealing of two fused rings to the existing cyclic systems shown below (Scheme 10). There is a similarity between the two cascades shown there – the initial 6-exo-cyclization makes a new radical that can be potentially trapped by the pendant phenyl group. Alkyne cyclization yield highly reactive vinyl radical that is capable of this addition reaction that affords a new five-membered ring[3a,5] whereas the highly delocalized π-radical formed in the *peri*-cyclization does not undergo the additional C-C bond forming reaction.

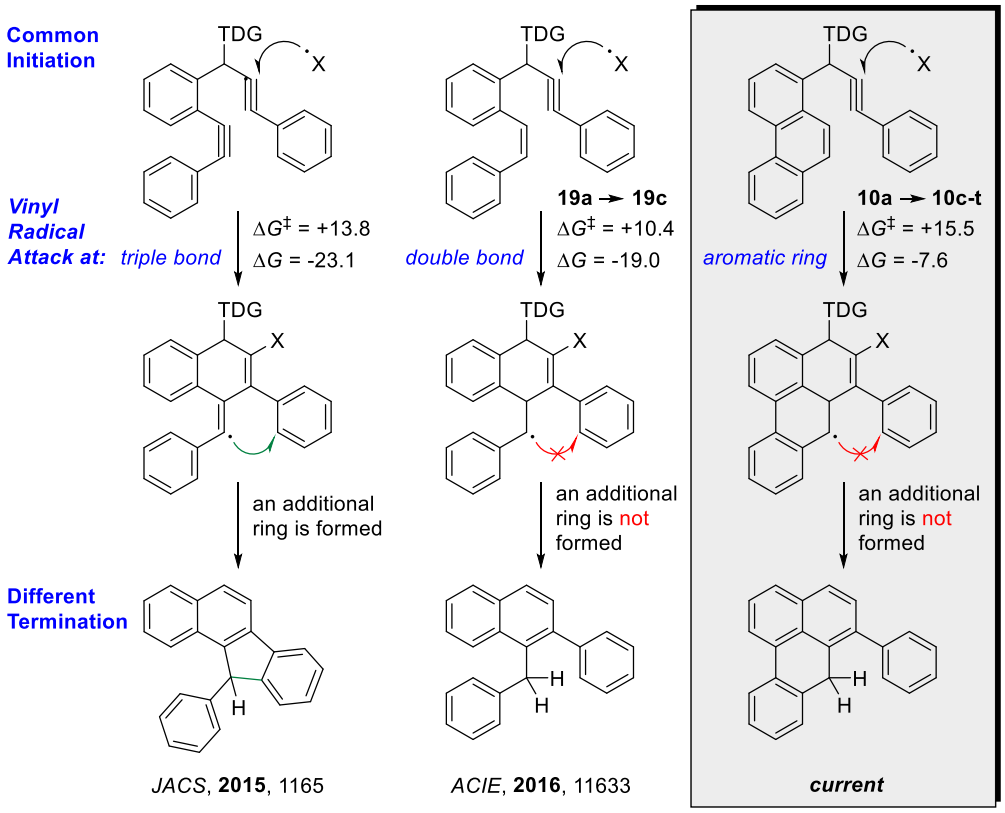

Scheme 10. Cascade product variation via alteration of vinyl radical target.

Conclusions

The theoretical study of *peri*-cyclization reactions revealed the significance of several factors when using vinyl radicals to expand aromatic systems. In particular, cyclization barriers are consistently lower for the *peri*-cyclizations that result in six-membered products, especially for those forming *cis*-products. Formation of the five-membered products from the same radical precursors via an ortho attack must overcome much higher barriers (~20-25 kcal/mol). These computational results rationalize the preferential formation of the 6-membered products under the experimental conditions. The aromaticity of the attacked ring is important in those cases where it is not masked by the steric factors.

The α- and β-substitution and the consequent vinyl radical stabilization have a large effect on reactivity, raising barriers and reaction energies. Introduction of the β-SnMe and α-phenyl groups stabilizes the vinyl radical and partially deactivates it towards the cyclization.

The key finding is unprecedented sensitivity of the *peri*-cyclization to the presence and spatial orientation of a "spectator" propargylic -OMe substituent. The two orientations of this substituent give rise to the *cis*- or *trans*-isomers of the cyclized product. Stability of these isomers is not dramatically different, and, sometimes, the cis-isomer is less stable. However, in every case the formation of the *cis*-product proceeds through a significantly (~2-5 kcal/mol) lower barrier than formation of the *trans*-products, The origin of this unexpected effect is clearly stereoelectronic – in the lower energy transition states, the $\sigma_{C\text{-}OMe}$ bond and the radical orbital are aligned with the "relay" C-Sn orbital whereas in the higher energy transition states the $\sigma_{C\text{-}OMe}$ bond is nearly orthogonal to the radical and the vinyl C-Sn bond. When the strength of the acceptor was increased by introducing a propargylic C-F bond, even larger effects on the cyclization barriers were observed. ***This dramatic stereoelectronic effect of a "spectator" group is a conceptually new tool for the control of rate and selectivity of radical reactions.***

Experimental Section

Computational Details. All computations were performed in *Gaussian 09* [15] with unrestricted M06-2X functional [16] due to its relatively accurate description of reaction and activation energies for a variety of chemical processes including radical reactions.[17] The LanL2DZ basis set was used for all atoms. Chemcraft 1.7[18] and CYLView[19] were used to render the orbitals and molecules. Frequency calculations were performed to confirm each stationary point as either a minimum or a first-order saddle point. Intrinsic Reaction Coordinates (IRC)[20] were determined

for the TS of interest. Natural Bond Orbital[21] (NBO) analysis was used on key intermediates and transition states.

Acknowledgments

We thank the National Science Foundation (CHE-1800329) for support of this research.

Supporting information

Geometries and energies for all calculated structures. Additional information about correlations between activation and reaction energies. This material is available free of charge via the Internet at http://pubs.acs.org

Conflicts of interest

There are no conflicts to declare.

References and Notes

(1) (a) Senese, A. D; Chalifoux, W. A. Nanographene and Graphene Nanoribbon Synthesis via Alkyne Benzannulations**.** *Molecules* **2019**, *24*, 118; (b) Yang, W; Monteiro, J. H. S. K; de Bettencourt-Dias, A; Catalano, V. J; Chalifoux, W. A. Pyrenes, Peropyrenes, and Teropyrenes: Synthesis, Structures, and Photophysical Properties. *Angew. Chem., Int. Ed.* **2016**, *55*, 10427–10430; (c) Yang, W; Bam, R; Catalano, V. J; Chalifoux, W. A. Highly Regioselective Domino Benzannulation Reaction of Buta-1,3-Diynes To Construct Irregular Nanographenes. *Angew. Chem., Int. Ed.* **2018**, *57*, 14773–14777; (d) Chernick, E. T; Tykwinski, R. R. Carbon-Rich Nanostructures: The Conversion of Acetylenes into Materials. *J. Phys. Org. Chem.* **2013**, *26*, 742–749. For selected non-annulative reactions of alkynes in the synthesis of polyaromatics, see: (e) Iyer, V. S; Wehmeier, M; Brand, J. D; Keegstra, M. A; Müllen, K. From Hexa-Peri-Hexabenzocoronene to "Superacenes." *Angew. Chem., Int. Ed. Engl.* **1997**, *36*, 1604–1607. (f) Feng, X; Pisula, W; Takase, M; Dou, X; Enkelmann, V; Wagner, M; Ding, N; Müllen, K. Synthesis, Helical Organization, and Fibrous Formation of C3 Symmetric Methoxy-Substituted Discotic Hexa-Peri-Hexabenzocoronene. *Chem. Mater.* **2008**, *20*, 2872–2874.

(2) (a) Yang, W; Chalifoux, W. A. Rapid π-Extension of Aromatics via Alkyne Benzannulations. *Synlett*, **2017**, *28*, 625-632; (b) Yang, W; Lucotti, A; Tommasini, M; Chalifoux, W. A. Bottom-Up Synthesis of Soluble and Narrow Graphene Nanoribbons Using Alkyne Benzannulations. *J. Am. Chem. Soc.* **2016**, *138*, 9137–9144; (c) Alabugin, I. V; Gold, B. "Two Functional Groups in One Package": Using Both Alkyne π-Bonds in Cascade Transformations. *J. Org. Chem.* **2013**, *78*, 7777–7784.

(3) (a) Pati, K; Gomes, G. P; Harris, T; Hughes, A; Phan, H; Banerjee, T; Hanson, K; Alabugin, I. V. Traceless Directing Groups in Radical Cascades: From Oligoalkynes to Fused Helicenes without Tethered Initiators. *J. Am. Chem. Soc.* **2015**, *137*, 1165–1180; (b) Byers, P. M; Alabugin, I. V. Polyaromatic Ribbons from Oligo-Alkynes via Selective Radical Cascade: Stitching Aromatic Rings with Polyacetylene Bridges. *J. Am. Chem. Soc.* **2012**, *134*, 9609–9614.

(4) Pati, K; Hughes, A. M; Phan, H; Alabugin, I. V. Exo-Dig Radical Cascades of Skipped Enediynes: Building a Naphthalene Moiety within a Polycyclic Framework. *Chem. - Eur. J.* **2014**, *20*, 390–393.

(5) Pati, K; Gomes, G. P; Alabugin, I. V. Combining Traceless Directing Groups with Hybridization Control of Radical Reactivity: From Skipped Enynes to Defect-Free Hexagonal Frameworks. *Angew. Chem., Int. Ed.* **2016**, *55*, 11633–11637.

(6) Tsvetkov, N. P; Gonzalez-Rodriguez, E; Hughes, A; Gomes, G. P; White, F. D; Kuriakose, F; Alabugin, I. V. Radical Alkyne Peri-Annulation Reactions for the Synthesis of Functionalized Phenalenes, Benzanthrenes, and Olympicene. *Angew. Chem., Int. Ed.* **2018**, *57*, 3651–3655.

(7) Pati, K; Michas, C; Allenger, D; Piskun, I; Coutros, P. S; Gomes, G. P; Alabugin, I. V. Synthesis of Functionalized Phenanthrenes via Regioselective Oxidative Radical Cyclization. *J. Org. Chem.* **2015**, *80*, 11706–11717.

(8) (a) Fischer, H; Radom, L. Factors Controlling the Addition of Carbon-Centered Radicals to Alkenes. *Angew. Chem., Int. Ed.* **2001**, *182*, 1340–1371. Examples for vinyl radicals: (b) Alabugin, I. V; Manoharan, M. Thermodynamic and Strain Effects in the Competition between 5-Exo-Dig

and 6-Endo-Dig Cyclizations of Vinyl and Aryl Radicals. *J. Am. Chem. Soc.* **2005**, *127*, 12583–12594; (c) Alabugin, I. V; Manoharan, M. 5-Endo-Dig Radical Cyclizations: "The Poor Cousins" of the Radical Cyclizations Family. *J. Am. Chem. Soc.* **2005**, *127*, 9534–9545; (d) Mohamed, R. K; Mondal, S; Gold, B; Evoniuk, C. J; Banerjee, T; Hanson, K; Alabugin, I. V. Alkenes as Alkyne Equivalents in Radical Cascades Terminated by Fragmentations: Overcoming Stereoelectronic Restrictions on Ring Expansions for the Preparation of Expanded Polyaromatics. *J. Am. Chem. Soc.* **2015**, *137*, 6335–6349.

(9) (a) Juaristi, E; Gomes, G. P; Terent'ev, A. O; Notario, R; Alabugin, I. V. Stereoelectronic Interactions as a Probe for the Existence of the Intramolecular α-Effect. *J. Am. Chem. Soc.* **2017**, *139*, 10799–10813; (b) Alabugin, I. V; Gilmore, K. Finding the Right Path: Baldwin "Rules for Ring Closure" and Stereoelectronic Control of Cyclizations. *Chem. Commun.* **2013**, *49*, 11246–11250; (c) Alabugin, I. V., *Stereoelectronic Effects: A Bridge Between Structure and Reactivity*, John Wiley & Sons Ltd, Chichester, UK, 2016; (d) Gilmore, K; Mohamed, R. K; Alabugin, I. V. The Baldwin Rules: Revised and Extended. *Wiley Interdiscip. Rev.: Comput. Mol. Sci.* **2016**, *6*, 487–514; (e) Vatsadze, S. Z; Loginova, Y. D; Gomes, G. P; Alabugin, I. V. Stereoelectronic Chameleons: The Donor–Acceptor Dichotomy of Functional Groups. *Chem. - Eur. J.* **2016**, *23*, 3225–3245. In radical processes: (f) Mondal, S; Gold, B; Mohamed, R. K; Alabugin, I. V. Design of Leaving Groups in Radical C-C Fragmentations: Through-Bond 2c-3e Interactions in Self-Terminating Radical Cascades. *Chem. - Eur. J.* **2014**, *20*, 8664–8669. In cyclic structures: (g) Gomes, G. P; Yaremenko, I. A; Radulov, P. S; Novikov, R. A; Chernyshev, V. V; Korlyukov, A. A; Nikishin, G. I; Alabugin, I. V; Terent'ev, A. O. Stereoelectronic Control in the Ozone-Free Synthesis of Ozonides. *Angew. Chem., Int. Ed.* **2017**, *56*, 4955–4959; (h) Yaremenko, I. A; Gomes, G. P; Radulov, P. S; Belyakova, Y. Y; Vilikotskiy, A. E; Vil, V. A; Korlyukov, A. A; Nikishin, G. I; Alabugin, I. V; Terent'Ev, A. O. Ozone-Free Synthesis of Ozonides: Assembling Bicyclic Structures from 1,5-Diketones and Hydrogen Peroxide. *J. Org. Chem.* **2018**, *83*, 4402–4426; (i) Vil', V. A; Gomes, G. P; Bityukov, O. V; Lyssenko, K. A; Nikishin, G. I; Alabugin, I. V; Terent'ev, A. O. Interrupted Baeyer–Villiger Rearrangement: Building A Stereoelectronic Trap for the Criegee Intermediate. *Angew. Chem., Int. Ed.* **2018**, *57*, 3372–3376.

(10) Effects of propargylic σ-acceptor on reactivity: (a) Gold, B; Dudley, G. B; Alabugin, I. V. Moderating Strain without Sacrificing Reactivity: Design of Fast and Tunable Noncatalyzed Alkyne-Azide Cycloadditions via Stereoelectronically Controlled Transition State Stabilization. *J. Am. Chem. Soc.* **2013**, *135*, 1558–1569; (b) Gold, B; Shevchenko, N. E; Bonus, N; Dudley, G. B; Alabugin, I. V. Selective Transition State Stabilization via Hyperconjugative and Conjugative Assistance: Stereoelectronic Concept for Copper-Free Click Chemistry. *J. Org. Chem.* **2012**, *77*, 75–89. Alignment of a remote group with a π -system: (c) Harris, T; Gomes, G. P; Ayad, S; Clark, R. J; Lobodin, V. V; Tuscan, M; Hanson, K; Alabugin, I. V. Twisted Cycloalkynes and Remote Activation of "Click" Reactivity. *Chem* **2017**, *3*, 629–640. Intramolecular interactions of the same Sn- and O-functionalities in radical fragmentations: (d) Harris, T; Gomes, G. P; Clark, R. J; Alabugin, I. V. Domino Fragmentations in Traceless Directing Groups of Radical Cascades: Evidence for the Formation of Alkoxy Radicals via C-O Scission. *J. Org. Chem.* **2016**, *81*, 6007–6017.

(11) Selected aromaticity-driven processes: (a) Messersmith, R. E; Yadav, S; Siegler, M. A; Ottosson, H; Tovar, J. D. Benzo[b]Thiophene Fusion Enhances Local Borepin Aromaticity in Polycyclic Heteroaromatic Compounds. *J. Org. Chem.* **2017**, *82*, 13440–13448; (b) Papadakis, R; Ottosson, H. The Excited State Antiaromatic Benzene Ring: A Molecular Mr Hyde? *Chem. Soc. Rev.* **2015**, *44*, 6472–6493; (c) Villaume, S; Fogarty, H. A; Ottosson, H. Triplet-State Aromaticity of 4nπ-Electron Monocycles: Analysis of Bifurcation in the π Contribution to the Electron Localization Function. *ChemPhysChem* **2008**, *9*, 257–264; (d) Evoniuk, C. J; Gomes, G. P; Ly, M; White, F. D; Alabugin, I. V. Coupling Radical Homoallylic Expansions with C-C Fragmentations for the Synthesis of Heteroaromatics: Quinolines from Reactions of o-Alkenylarylisonitriles with Aryl, Alkyl, and Perfluoroalkyl Radicals. *J. Org. Chem.* **2017**, *82*, 4265–4278; (e) Peterson, P. W; Mohamed, R. K; Alabugin, I. V. How to Lose a Bond in Two Ways - The Diradical/Zwitterion Dichotomy in Cycloaromatization Reactions. *Eur. J. Org. Chem.* **2013**, *2013*, 2505–2527; (f) Mohamed, R. K; Mondal, S; Jorner, K; Delgado, T. F; Lobodin, V. V; Ottosson, H; Alabugin, I. V. The Missing C1-C5Cycloaromatization Reaction: Triplet State Antiaromaticity Relief and Self-Terminating Photorelease of Formaldehyde for Synthesis of Fulvenes from Enynes. *J. Am. Chem. Soc.* **2015**, *137*, 15441–15450; (g) Babinski, D. J; Bao, X; El Arba, M; Chen, B; Hrovat, D. A;

Borden, W. T; Frantz, D. E. Synchronized Aromaticity as an Enthalpic Driving Force for the Aromatic Cope Rearrangement. *J. Am. Chem. Soc.* **2012**, *134*, 16139–16142.

(12) Chen, Z; Wannere, C. S; Corminboeuf, C; Puchta, R; Schleyer, P. R. Nucleus-Independent Chemical Shifts (NICS) as an Aromaticity Criterion. *Chem. Rev.* **2005**, *105*, 3842–3888.

(13) (a) Schleyer, P. R; Wu, J. I; Cossío, F. P; Fernández, I. Aromaticity in Transition Structures. *Chem. Soc. Rev.* **2014**, *43*, 4909–4921; (b) Schleyer, P. R; Manoharan, M; Wang, Z. X; Kiran, B; Jiao, H; Puchta, R; Van Eikema Hommes, N. J. R. Dissected Nucleus-Independent Chemical Shift Analysis of π-Aromaticity and Antiaromaticity. *Org. Lett.* **2001**, *3*, 2465–2468; (c) Gogonea, V; Schleyer, P. R; Schreiner, P. R. Consequences of Triplet Aromaticity in 4nπ-Electron Annulenes: Calculation of Magnetic Shieldings for Open-Shell Species. *Angew. Chem., Int. Ed.* **1998**, *37*, 1945–1948; (d) Rosenberg, M; Dahlstrand, C; Kilså, K; Ottosson, H. Excited State Aromaticity and Antiaromaticity: Opportunities for Photophysical and Photochemical Rationalizations. *Chem. Rev.* **2014**, *114*, 5379–5425; (e) Stanger, A. Nucleus-Independent Chemical Shifts (NICS): Distance Dependence and Revised Criteria for Aromaticity and Antiaromaticity. *J. Org. Chem.* **2006**, *71*, 883–893; (f) Gershoni-Poranne, R; Stanger, A. Magnetic Criteria of Aromaticity. *Chem. Soc. Rev.* **2015**, *44*, 6597–6615; (g) Gershoni-Poranne, R. Piecing It Together: An Additivity Scheme for Aromaticity Using NICS-XY Scans. *Chem. - Eur. J.* **2018**, *24*, 4165–4172; (h) Corminboeuf, C; Heine, T; Weber, J. Evaluation of Aromaticity: A New Dissected NICS Model Based on Canonical Orbitals. *Phys. Chem. Chem. Phys.* **2003**, *5*, 246–251; (i) Van Speybroeck, V; Hemelsoet, K; Waroquier, M; Marin, G. B. Reactivity and Aromaticity of Polyaromatics in Radical Cyclization Reactions. *Int. J. Quantum Chem.* **2004**, *96*, 568–576.

(14) The Curtin-Hammett principle applies when barrier of reactions are considerably higher than the barriers for the interconversion of the two reacting species. In the present case, the calculated cyclization barrier heights (8-17 kcal/mol) significantly exceed the typical barriers for the rotation around single bonds.

(15) Frisch, M. J., et. al., Gaussian 09, Revision B.01; Gaussian: Wallingford, CT, 2009. Full reference in the ESI.

(16) (a) Zhao, Y; Truhlar, D. G. The M06 Suite of Density Functionals for Main Group Thermochemistry, Thermochemical Kinetics, Noncovalent Interactions, Excited States, and Transition Elements: Two New Functionals and Systematic Testing of Four M06-Class Functionals and 12 Other Functionals. *Theor. Chem. Acc.* **2008**, *120*, 215–241; (b) Zhao, Y; Truhlar, D. G. Density Functionals with Broad Applicability in Chemistry. *Acc. Chem. Res.* **2008**, *41*, 157–167.

(17) Zhao, Y; Truhlar, D. G. How Well Can New-Generation Density Functionals Describe the Energetics of Bond-Dissociation Reactions Producing Radicals? *J. Phys. Chem. A* **2008**, *112*, 1095–1099.

(18) http://www.chemcraftprog.com.

(19) Legault, C. Y., CYLview, 1.0b, Université de Sherbrooke, Québec, Montreal, Canada, 2009, http://www.cylview.org.

(20) Fukui, K. The Path of Chemical Reactions - The IRC Approach. *Acc. Chem. Res.* **1981**, *14*, 363–368.

(21) (a) Weinhold, F; Landis, C. R; Glendening, E. D. What Is NBO Analysis and How Is It Useful? *Int. Rev. Phys. Chem.* **2016**, *35*, 399–440; (b) Weinhold, F. in Schleyer, P. R., *Encyclopedia of Computational Chemistry*: Wiley: New-York, 1998, **3**, 1792; (Selected recent applications of NBO analysis towards organic structure and reactivity: (c) Podlech, J. Stereoelectronic Effects in α-Carbanions of Conformationally Constrained Sulfides, Sulfoxides, and Sulfones. *J. Phys. Chem. A* **2010**, *114*, 8480–8487; (d) Freitas, M. P. Simultaneous Gauche and Anomeric Effects in α-Substituted Sulfoxides. *J. Org. Chem.* **2012**, *77*, 7607–7611; (e) Greenway, K. T; Bischoff, A. G; Pinto, B. M. Probing Hyperconjugation Experimentally with the Conformational Deuterium Isotope Effect. *J. Org. Chem.* **2012**, *77*, 9221–9226; (f) Juaristi, E; Notario, R. Theoretical Examination of the S-C-P Anomeric Effect. *J. Org. Chem.* **2015**, *80*, 2879–2883; (g) Gomes, G. P; Vil, V; Terent'Ev, A; Alabugin, I. V. Stereoelectronic Source of the Anomalous Stability of

Bis-Peroxides. *Chem. Sci.* **2015**, *6*, 6783–6791; (h) Vidhani, D. V; Krafft, M. E; Alabugin, I. V. Gold(I)-Catalyzed Allenyl Cope Rearrangement: Evolution from Asynchronicity to Trappable Intermediates Assisted by Stereoelectronic Switching. *J. Am. Chem. Soc.* **2016**, *138*, 2769–2779.